



## Effect of side chain position on solar cell performance in cyclopentadithiophene-based copolymers

Sang Kyu Lee <sup>a</sup>, Jung Hwa Seo <sup>b</sup>, Nam Sung Cho <sup>c</sup>, Shinuk Cho <sup>d,\*</sup>

<sup>a</sup> Energy Materials Research Center, Korea Research Institute of Chemical Technology (KRICT), Daejeon 305-600, Republic of Korea

<sup>b</sup> Department of Materials Physics, Dong-A University, Busan 604-714, Republic of Korea

<sup>c</sup> Electronics and Telecommunications Research Institute (ETRI), 161 Gajeong-dong, Yuseong-gu, Daejeon 305-350, Republic of Korea

<sup>d</sup> Department of Physics and EHSRC, University of Ulsan, Ulsan 680-749, Republic of Korea

### ARTICLE INFO

#### Article history:

Received 2 November 2011

Received in revised form 2 April 2012

Accepted 5 April 2012

Available online 15 April 2012

#### Keywords:

Donors–acceptors conjugated copolymer

Substituted side chain

Polymer solar cells

### ABSTRACT

The photovoltaic properties of a series of low band-gap conjugated copolymers, in which alkyl side chains were substituted at various positions, were investigated using donor–acceptor (D–A) conjugated copolymers consisting of a cyclopentadithiophene derivative and dithienyl-benzothiadiazole. The base polymer, which has no alkyl side chains, yielded promising power conversion efficiency of 3.8%. Polymers with alkyl side chains, however, exhibited significantly decreased performance. In addition, the effects of processing additive became negligible. The results indicate that substituted side chains, which were introduced to improve solubility, critically affected the optical and electronic properties of D–A conjugated copolymers. Furthermore, the position of the side chain was also very important for controlling the morphological properties of the D–A conjugated copolymers.

© 2012 Elsevier B.V. All rights reserved.

### 1. Introduction

Conjugated copolymers with electron donor (D)–acceptor (A) units in the repeat unit have drawn considerable attention for their use in bulk-heterojunction (BHJ) photovoltaic cells. These conjugated copolymers exhibit intra-molecular charge transfer (ICT) over the electron-donating and electron-accepting segments, which can lead to low-band-gap conjugated polymers that efficiently harvest the solar spectrum [1–4].

A number of D–A copolymers have been generated and subsequently characterized [1–6]. The most popular D–A copolymer structure is the donor–thiophene–acceptor–thiophene structure (DDAD type) [2–7]. However, because they convey solubility only from the conjugated core units, DDAD type copolymers have relatively low solubility if they have a high molecular weight ( $M_w$ ) [3,7–9]. Introducing alkyl side chains at the thiophene unit is the simplest approach to improving the solubility of DDAD type copolymers. In a previous report, we investigated the effects of the position of substituted alkyl side chains on the transport properties in field-effect transistors [10]. Although the substituted side chains conferred better solubility of the D–A conjugated copolymers, we found that the intrinsic charge transport properties were significantly altered due to a disturbance in ICT between the donor and acceptor segments.

In the present study, the photovoltaic properties of a series of low band-gap conjugated copolymers with alkyl side chains substituted at various positions was investigated using donor–acceptor (D–A) conjugated copolymers consisting of a cyclopentadithiophene (CPDT) derivative and dithienyl-benzothiadiazole (DTBT) (see Fig. 1).

### 2. Experimental details

The CPDT-based copolymers were synthesized through a Stille coupling reaction of a distannyl derivative of CPDT and alkyl chain-substituted dithienyl-benzothiadiazole derivatives. Tri(dibenzylideneacetone)dipalladium ( $Pd_2(dba)_3$ ) was used as the catalyst and tri(*o*-tolyl)phosphine as the ligand [6,10]. Molecular weights were determined by gel permeation chromatography in chlorobenzene using polystyrene standards and they were found to be in the range of 7.0 kDa–12 kDa with a polydispersity index of 1.3–2.0. The polymers are soluble in common organic solvents, such as tetrahydrofuran, chloroform, and toluene.

BHJ solar cells were fabricated on an indium tin oxide (ITO)-coated glass substrate. Poly(3,4-ethylenedioxythiophene):poly(styrenesulfonate) (PEDOT:PSS) was spin-cast in air at 5000 rpm for 40 s onto the pre-cleaned ITO/glass. The blend solutions of polymer:PC<sub>71</sub>BM (1:1.5 w/w) in chlorobenzene with 10 mg/mL were prepared. The solutions were subsequently deposited by spin casting onto the PEDOT:PSS/ITO/glass after stirring the solutions on a hot plate at 100 °C for overnight. After active layer deposition, the films were dried on a hot plate and stabilized at 80 °C for 30 min. Al metal was then deposited by thermal evaporation in high vacuum ( $4 \times 10^{-4}$  Pa). Prior to

\* Corresponding author.

E-mail address: [sucho@ulsan.ac.kr](mailto:sucho@ulsan.ac.kr) (S. Cho).

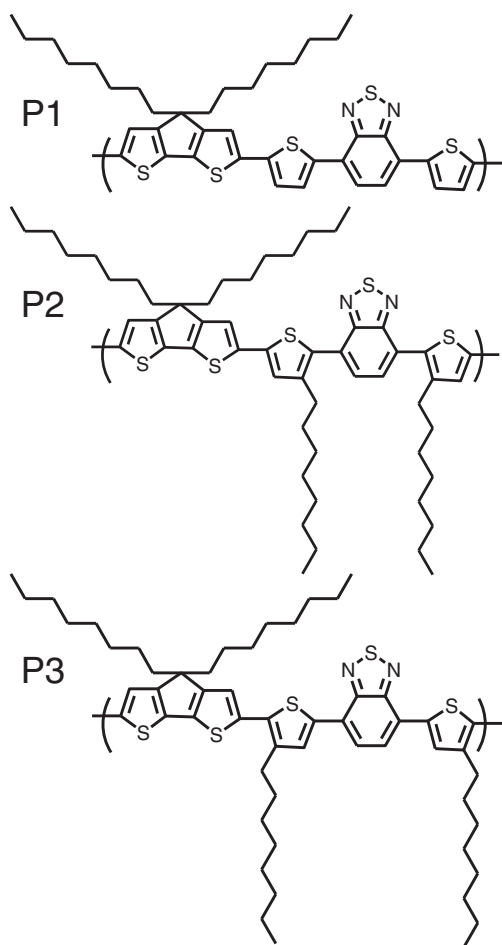


Fig. 1. Chemical structures of the polymers.

cathode metal deposition, a 1 nm lithium fluoride (LiF) layer was deposited.

Current–voltage characteristic curves were measured using a Keithley 2400 source meter. Solar cell performance was characterized using an AM 1.5 G solar simulator (100 mW/cm<sup>2</sup>). An aperture was used on top of the cell to eliminate extrinsic effects such as cross talk, wave guiding, and shadow effect. Incident-photon-to-electron conversion efficiency (IPCE) spectra were measured using a solar cell spectral response measurement system (PV Measurements, Inc., Model QEW 7). Tapping mode atomic force microscopy (AFM) images were obtained using a Multimode microscope with a Nanoscope IIIa controller (Veeco).

### 3. Results and discussion

Fig. 1 shows the chemical structures of the D–A conjugated copolymers studied in this work. Based on the original copolymer, poly[2,6-(4,4-bis(2-octyl)-4*H*-cyclopenta-[2,1-*b*:3,4-*b'*]dithiophene)-*alt*-4,7-bis(thiophene-2-yl)benzo-2,1,3-thiadiazole] (PCPDT-TBTT, P1), alkyl chains were introduced in a tail–tail configuration for the poly[2,6-(4,4-bis(2-octyl)-4*H*-cyclopenta-[2,1-*b*:3,4-*b'*]dithiophene)-*alt*-4,7-bis(4-octyl-thiophene-2-yl)benzo-2,1,3-thiadiazole] (PCPDT-tOTBTOT, P2). For the poly[2,6-(4,4-bis(2-octyl)-4*H*-cyclopenta-[2,1-*b*:3,4-*b'*]dithiophene)-*alt*-4,7-bis(3-octyl-thiophene-2-yl)benzo-2,1,3-thiadiazole] (PCPDT-hhOTBTOT, P3), alkyl chains were introduced in a head–head configuration. The synthetic details and chemical properties of these copolymers are described elsewhere [10].

The UV–vis absorption spectra of the three polymers are shown in Fig. 2(a). All absorption spectra are typical of D–A conjugated

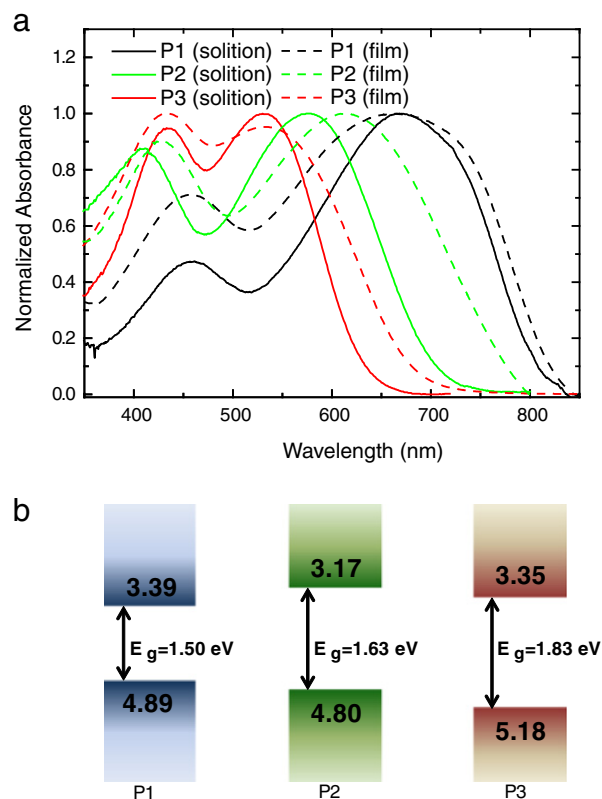
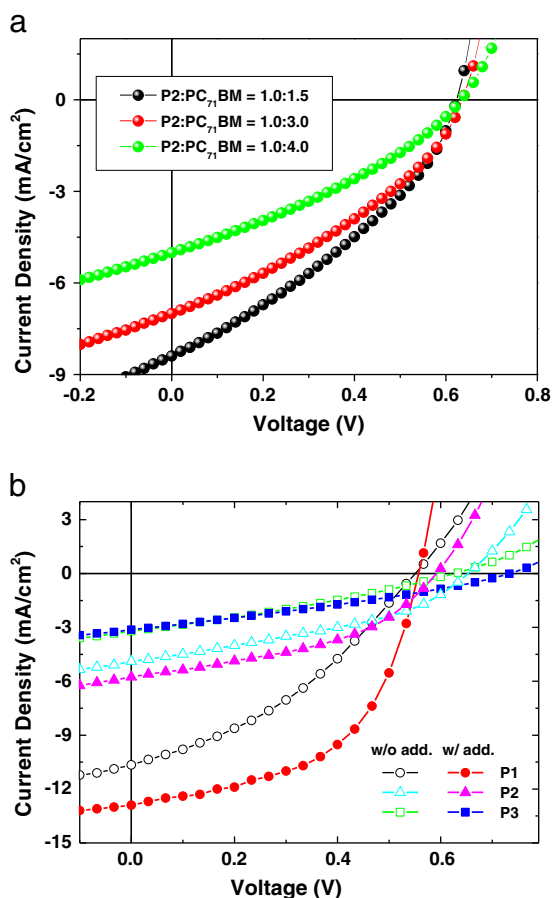


Fig. 2. (a) Absorption spectra of the polymers in chloroform (solid line) and in the solid state (dashed line). (b) Energy levels for the polymers.

copolymers that show camel-back absorption spectra with two distinct broad absorption peaks. The short-wavelength absorption peaks are attributed to a delocalized  $\pi$ – $\pi^*$  transition in the polymer chains while the long-wavelength absorption peaks are attributed to a localized transition between the D–A–D charge transfer states [11,12]. Although all the absorption spectra in Fig. 2 are similar in shape, substituted side chains on the thiophene moiety induced blue shifts in the absorption spectrum. The origin of the low band-gap properties in D–A conjugated copolymers is understood to be based on ICT. Therefore, we attributed the blue shifted absorption spectra for P2 and P3 to weaker ICT resulting from small alterations in the main chain configuration due to the alkyl side chains. Energy level diagrams for the three polymers are depicted in Fig. 2(b).

The current–voltage characteristics of the BHJ solar cells are shown in Fig. 3. BHJ solar cells were fabricated with a structure of ITO/PEDOT:PSS/polymer:PC<sub>71</sub>BM/LiF/Al. Initially, to find the optimum blend ratio, devices were prepared and tested with various mixture ratios (1:1.5, 1:3, and 1:4, w/w). As shown in Fig. 3(a), the performance depends on the amount of PC<sub>71</sub>BM (see Table 1). The 1:1.5 ratio P2:PC<sub>71</sub>BM yields power conversion efficiency (PCE) of 1.80% with short circuit current density ( $J_{SC}$ ) of 8.40 mA/cm<sup>2</sup>, an open circuit voltage ( $V_{OC}$ ) of 0.62, a fill factor (FF) of 0.34, while device with 1:3 ratio resulted PCE = 1.56% with  $J_{SC}$  = 7.01 mA/cm<sup>2</sup>,  $V_{OC}$  = 0.64 V, FF = 0.35. In the case of 1:4 ratio solar cell, the performance was more decreased in PCE = 1.04% with  $J_{SC}$  = 5.01 mA/cm<sup>2</sup>,  $V_{OC}$  = 0.63 V, FF = 0.33. We conclude that the optimum P2:PC<sub>71</sub>BM mixture ratio is 1:1.5. P1 and P3 polymer also showed the highest performance at same blend ratio.

To enhance solar cell performance more, we applied a processing additive using 2% 1,8-diiodooctane. Under standard AM 1.5 G conditions (100 mW/cm<sup>2</sup>), P1:PC<sub>71</sub>BM (with 1,8-diiodooctane) was the best performing solar cell. This cell exhibited a PCE = 3.8% with  $J_{SC}$  = 12.9 mA/cm<sup>2</sup>,  $V_{OC}$  = 0.56 V, and FF = 0.51. Detailed solar cell



**Fig. 3.** (a) Current density ( $J$ )-voltage ( $V$ ) characteristics (under simulated AM 1.5 G radiation at  $100 \text{ mW/cm}^2$ ) for a P2 polymer:PC<sub>71</sub>BM with various blend ratios. (b)  $J$ - $V$  characteristics for a series of polymers:PC<sub>71</sub>BM with and without 1,8-diiodooctane additive.

performance data are listed in Table 2 and the measured IPCE is presented in Fig. 4. All solar cells fabricated with P2 or P3, which have alkyl side chains, exhibited significantly decreased photovoltaic parameters. Furthermore, in these solar cells, the effects of the processing additive were negligible. The P3:PC<sub>71</sub>BM solar cell exhibited poor performance that is explained by the low charge mobility ( $\sim 10^{-6} \text{ cm}^2/\text{V s}$ ) of P3 and a blue shifted absorption spectrum. The P2:PC<sub>71</sub>BM solar cell had significantly suppressed solar cell performance. This result was unexpected since the P2 field-effect mobility of  $1.8 \times 10^{-3} \text{ cm}^2/\text{V s}$  is similar to that of P1 ( $4.9 \times 10^{-3} \text{ cm}^2/\text{V s}$ ) [10].

Interestingly, although the P1:PC<sub>71</sub>BM solar cell showed the highest PCE value, the  $V_{\text{OC}}$  value of P1:PC<sub>71</sub>BM solar cell is relatively lower than that of P2:PC<sub>71</sub>BM and P3:PC<sub>71</sub>BM solar cells. The  $V_{\text{OC}}$  value expected from the gap between HOMO of polymer and LUMO of fullerene is especially observed when the BHJ layer has better morphology. For instance, the  $V_{\text{OC}}$  values of P3HT:PCBM are exhibited at 0.4 V to 0.7 V in their variable morphologies even though same material is used. From this similar reason, the trend of  $V_{\text{OC}}$  value of cyclopentadithiophene-based copolymers could be hidden on the

**Table 1**  
The photovoltaic properties of the devices with various P2/PC<sub>71</sub>BM blend ratios.

P2:PC <sub>71</sub> BM ratio	$V_{\text{OC}}$ (V)	$J_{\text{sc}}$ (mA/cm <sup>2</sup> )	FF	PCE
1:1.5	0.62	8.40	0.34	1.80
1:3	0.64	7.01	0.35	1.56
1:4	0.63	5.01	0.33	1.04

**Table 2**

Photovoltaic performance of the devices based on the blend of P1, P2 and P3 polymers with PC<sub>71</sub>BM (1:1.5 w/w) under AM 1.5 G illumination.

	$V_{\text{OC}}$ (V)	$J_{\text{sc}}$ (mA/cm <sup>2</sup> )	FF	PCE	Additive
PCPDT-TBTT (P1)	0.53	10.7	0.36	2.1	0
	0.56	12.9	0.51	3.8	2
PCPDT-ttOTBTOT (P2)	0.64	4.8	0.39	1.2	0
	0.62	8.40	0.34	1.8	2
PCPDT-hhOTBTOT (P3)	0.62	3.2	0.30	0.6	0
	0.72	3.1	0.30	0.7	2

affection by the different morphology. In general, not only the  $V_{\text{OC}}$ , all parameters determining the performance of BHJ solar cells are strongly correlated to the nanomorphology of the film [2,13–15]. Differences in the BHJ morphology presumably play a crucial role in solar cell devices.

Fig. 5 shows the height images of the P1:PC<sub>71</sub>BM, P2:PC<sub>71</sub>BM, and P3:PC<sub>71</sub>BM films recorded by AFM. For the P1:PC<sub>71</sub>BM film without additive, the AFM height image exhibited a rough film morphology consisting of oval shaped grains. Apparently, these valleys characterize an uneven surface with a root-mean-square (rms) roughness of 1.45 nm for a  $2 \times 2 \mu\text{m}^2$  scan area. In contrast, after processing with additive, the AFM topography changed to a slightly smoother film (rms: 1.37 nm) and smaller granules. Such modified film morphology probably improved solar cell performance.

The oval shaped grains of the P2:PC<sub>71</sub>BM film disappeared due to the slightly enhanced solubility caused by the substituted alkyl side chains. In addition, film smoothness of the P2:PC<sub>71</sub>BM film (rms: 0.45 nm) is significantly improved compared to P1:PC<sub>71</sub>BM film. However, the P2:PC<sub>71</sub>BM film still exhibited aggregate morphology on AFM. This aggregate morphology did not improve at all with processing additive. Only the surface roughness improved slightly, from 0.45 nm to 0.33 nm, which resulted in slightly enhanced PCE values, from 1.2% to 1.8%. However, the photovoltaic performance of the P2 polymer is still limited by its aggregate morphology. Note that the error of rms values ranges in  $\pm 0.5 \text{ nm}$ . Therefore, the roughness of polymer:PC<sub>71</sub>BM films could be a minor parameter to determine device performance here.

Interestingly, alkyl side chains located at different positions of a thiophene moiety can significantly change the film morphology. The AFM topography of a P3:PC<sub>71</sub>BM film shows a uniform film surface with a low rms value of 0.52 nm, indicating the enhanced solubility caused by alkyl side chains in a head-head configuration. Although the P3:PC<sub>71</sub>BM film with additive shows better surface features rather than that without additive, this enhanced morphology could not overcome the intrinsic disadvantages (low

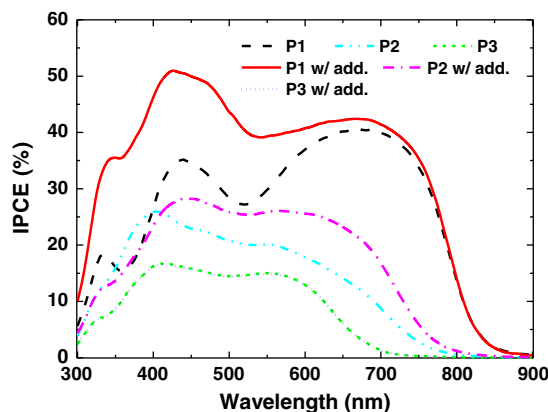


**Fig. 4.** IPCE spectra of polymer BHJ solar cells composed of polymer:PC<sub>71</sub>BM with and without 1,8-diiodooctane.

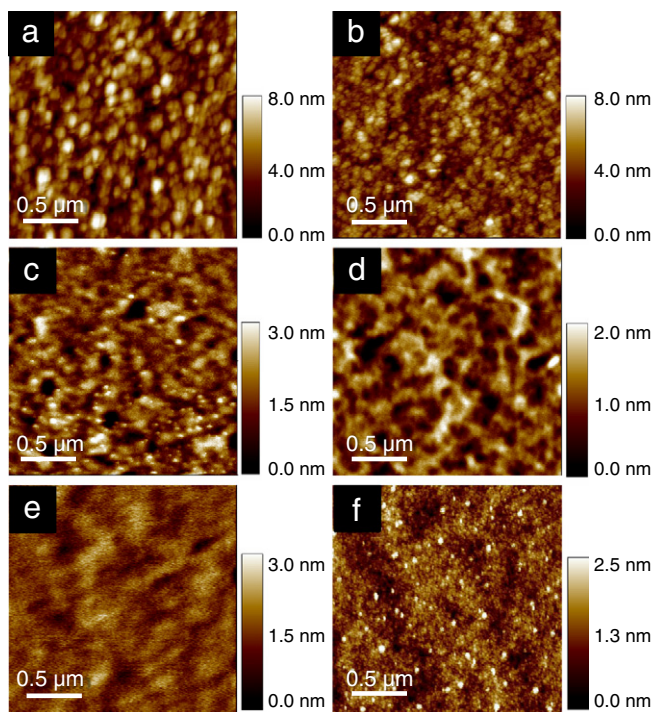


**Fig. 5.** AFM topography of films cast from P1:PC<sub>71</sub>BM without (a) and with (b) the use of 1,8-diiodooctane, P2:PC<sub>71</sub>BM without (c) and with (d) the use of 1,8-diiodooctane, and P3:PC<sub>71</sub>BM without (e) and with (f) the use of 1,8-diiodooctane.

mobility and inefficient harvesting of the solar spectrum) of the material itself.

#### 4. Conclusions

In conclusion, we have investigated the effects of the position of substituted alkyl side chains on the photovoltaic properties of DDAD type copolymers based on CPDT derivatives and DTBT. The solar cell performance of the P1 base polymer, which has no alkyl side chains, resulted in a PCE of 3.8% with processing additive. However, for P2 and P3, which have alkyl side chains, the photovoltaic parameters significantly decreased and the effects of processing additive became negligible. We attributed the low performance of P3

to low mobility and inefficient harvesting of the solar spectrum. The suppressed solar cell performance of the P2 polymer might have resulted from its aggregate morphology. These results indicated that the introduction of substituted side chains to improve solubility also critically affected the optical and electronic properties of D–A conjugated copolymers. Furthermore, the position of the side chain is very important for controlling the morphological properties of D–A conjugated copolymers.

#### Acknowledgments

This research was supported by the Basic Science Research Program (2011-0009148) and the Priority Research Centers Program (2009-0093818) through the National Research Foundation of Korea (NRF) funded by the Ministry of Education, Science, and Technology (MEST). The study in the Korea Research Institute of Chemical Technology was supported by the Converging Research Center Program through the Ministry of Education, Science, and Technology (2010K000970), Republic of Korea.

#### References

- [1] H.-Y. Chen, J.H. Hou, S.Q. Zhang, Y. Liang, G.W. Yang, Y. Yang, L.P. Yu, Y. Wu, G. Li, *Nat. Photonics* 3 (2009) 649.
- [2] S.H. Park, A. Roy, S. Beaupre, S. Cho, N. Coates, J.S. Moon, D. Moses, M. Leclerc, K. Lee, A.J. Heeger, *Nat. Photonics* 3 (2009) 297.
- [3] S.K. Lee, W.-H. Lee, J.M. Cho, S.J. Park, J.-U. Park, W.S. Shin, J.-C. Lee, I.-N. Kang, S.-J. Moon, *Macromolecules* 44 (2011) 5994.
- [4] S.J. Park, J.M. Cho, W.-B. Byun, J.-C. Lee, W.S. Shin, I.-N. Kang, S.-J. Moon, S.K. Lee, *J. Polym. Sci., Part A: Polym. Chem.* 49 (2011) 4416.
- [5] S.K. Lee, J.M. Cho, Y. Goo, W.S. Shin, J.-C. Lee, W.-H. Lee, I.-N. Kang, H.-K. Shim, S.-J. Moon, *Chem. Commun.* 47 (2011) 1791.
- [6] S.K. Lee, I.-N. Kang, J.-C. Lee, W.S. Shin, W.-W. So, S.-J. Moon, *J. Polym. Sci., Part A: Polym. Chem.* 49 (2011) 3129.
- [7] N. Blouin, A. Michaud, M. Leclerc, *Adv. Mater.* 19 (2007) 2295.
- [8] N. Blouin, A. Michaud, D. Gendron, S. Wakim, E. Blair, R. Neagu-Plesu, M. Belletete, G. Durocher, Y. Tao, M. Leclerc, *J. Am. Chem. Soc.* 130 (2008) 732.
- [9] H. Yi, S. Al-Faifi, A. Iraqi, D.C. Watters, J. Kingsley, D.G. Lidzey, *J. Mater. Chem.* 21 (2011) 13649.
- [10] S.K. Lee, S. Cho, M. Tong, J.H. Seo, A.J. Heeger, *J. Polym. Sci., Part A: Polym. Chem.* 49 (2011) 1821.
- [11] K.G. Jespersen, W.J.D. Beenken, Y. Zaushitsyn, A. Yartsev, M. Andersson, T. Pullerits, V. Sundström, *J. Chem. Phys.* 121 (2004) 12613.
- [12] A. Gadisa, W. Mammo, L.M. Andersson, S. Admassie, F. Zhang, M.R. Andersson, O. Inganäs, *Adv. Funct. Mater.* 17 (2007) 3836.
- [13] S.K. Lee, N.S. Cho, S. Cho, S.-J. Moon, J.K. Lee, G.C. Bazan, *J. Polym. Sci., Part A: Polym. Chem.* 47 (2009) 6873.
- [14] J. Kim, S.H. Kim, I.H. Jung, E. Jeong, Y. Xia, S. Cho, I.-W. Hwang, K. Lee, H. Suh, H.-K. Shim, H.Y. Woo, *J. Mater. Chem.* 20 (2010) 1577.
- [15] S.D. Oosterhout, M.M. Wienk, S.S. van Bavel, R. Thiedmann, L.J.A. Koster, J. Gilot, J. Loos, V. Schmidt, R.A.J. Janssen, *Nat. Mater.* 8 (2009) 818.